In Situ Scanning Tunneling Microscopy of the Anodic Oxidation of Highly Oriented Pyrolytic Graphite Surfaces

Andrew A. Gewirth and Allen J. Bard*

Department of Chemistry, The University of Texas at Austin, Austin, Texas 78712 *(Received: July 5, 1988)*

The scanning tunneling microscope (STM) was used to follow the in situ anodic oxidation of highly oriented pyrolytic graphite (HOPG) in 0.1 M H_2SO_4. Prior to electrochemical cycling, the HOPG surface appeared atomically flat and atomic structure was observed with the surface under potential control. Cycling between 0.0 and 1.8 V vs AgQRE (silver wire quasi-reference electrode) resulted in the formation of an amorphous graphite oxide overlayer structure exhibiting reduced barrier heights to tunneling, which grew anisotropically into the basal graphite plane. With continued cycling this structure completely covered the surface, forming a rough amorphous film. These images suggest that graphitic oxide overlayer formation occurs according to a nucleation and growth mechanism.

We report here studies of the surface of highly oriented pyrolytic graphite (HOPG) at atomic resolution with the scanning tunneling microscope (STM) with the sample immersed in an aqueous solution and under potential control. We also describe the effect of anodic oxidation of the HOPG sample in dilute sulfuric acid on the surface topography and composition.

The introduction of the STM[1] has provided a new approach to studies of solid surfaces in different media with a resolution to the atomic scale and investigations of the effect of chemical and electrochemical processes on the surface structure. Several STM studies of surface morphology in aqueous solutions have appeared and have been recently reviewed.[2] One of the earliest studies, following the initial observation of atomic resolution structure in aqueous environments,[3] monitored the in situ electrochemical deposition of Ag on graphite.[4] The STM has also been used to image Ag,[5] Au,[6] and Pt[7] surfaces in solution and to show nanometer scale features on Pt,[8] Ni,[9] and graphite[10] surfaces while these surfaces were under potential control. Recently, nanometer scale features on Au(111) single crystals under potential control have been observed,[11] but, to date, no atomic resolution has been reported for surfaces in aqueous environment under potential control.

The anodic oxidation of carbon surfaces has been the focus of substantial attention[12] not only because of the scientific and analytical interest in carbon surfaces but also because oxidation of HOPG to form graphitic oxide has been proposed for use as an electrochemical energy storage system.[13] While a number of spectroscopic studies of carbon electrodes following oxidation have appeared,[14] microscopic correlation of the oxidized overlayer with the underlying graphite structure remains to be elucidated.

Experimental Section

The STM used in this study represents an evolution of the designs first developed by Kaiser and Jaklevic[15] and Hansma and co-workers[16] and is shown in Figure 1. The sample was bolted to a glass plate with bolts and clips made from Kel-F and Teflon, respectively. The plate was pressed against three stainless steel threaded rods with Viton O-rings. The threads were protected from the solution by small glass cups glued to the sample holder. The XYZ translator was fabricated from a piezoceramic tube,[17] while the tip was placed in a small holder, which was glued to a Macor standoff fixed to the tube and fastened with a set screw. The tube and holder were wrapped with Parafilm, and the tip–tip holder junction was sealed with silicon stopcock grease to isolate them from the solution. A piezoceramic block under the tube, actuated with a 30-s time constant, provided active compensation for thermal drift.[18] Coarse approach of the tip to the sample was first accomplished by rotating two of the threaded rods until the sample was within 1 mm of the tip. The third threaded rod was then withdrawn slowly by a stepping motor driving a reduction gear until tunneling current was sensed. The STM was placed on a 30-kg plate suspended from the ceiling with rubber cords.[19] Because the sample and sample holder are immersed into the solution, this design allows the use of substantially larger electrolyte volumes (ca. 40 mL) than those previously used in other high-resolution instruments (ca. 0.2 mL). Large volumes are useful because this minimizes changes in electrolyte concentration over the duration of the experiment, allows one to use larger, more readily replaceable reference and auxiliary electrodes, and makes it easier to seal the cell and degas the solution.

The STM electronics used were standard, with the exception that a potentiostat was used to hold the sample at virtual ground. Bias was applied through the tip, and the tunneling current was measured here as well by using a subtraction circuit[20] to remove the contribution from the applied voltage. Potential measurements were made relative to a silver wire quasi-reference electrode (AgQRE), with the voltage sweep provided by a PAR Model 175

(1) (a) Binnig, G.; Rohrer, H. *Helv. Phys. Acta* **1982**, *55*, 726. (b) Binnig, G.; Rorher, H.; Gerber, Ch.; Weibel, E. *Phys. Rev. Lett.* **1982**, *49*, 57.
(2) Sonnenfeld, R.; Schneir, J.; Hansma, P. K. In *Modern Aspects of Electrochemistry*; White, R. E., Bockris, J. O'M., Conway, B. E., Eds., Vol. 19, in press.
(3) Sonnenfeld, R.; Hansma, P. K. *Science* **1986**, *232*, 211.
(4) Sonnenfeld, R.; Schardt, B. C. *Appl. Phys. Lett.* **1986**, *49*, 1172.
(5) Morita, S.; Otswka, I.; Okada, T.; Yokoyama, H.; Iwasaki, T.; Mikoshiba, N. *Jpn. J. Appl. Phys.* **1987**, *27*, L1853.
(6) (a) Drake, B.; Sonnenfeld, R.; Schneir, J.; Hansma, P. K. *Surf. Sci.* **1987**, *181*, 92. (b) Lindsay, S. M.; Barris, B. *J. Vac. Sci. Technol., A* **1988**, *6*, 544. (c) Schneir, J.; Marti, O.; Remmers, G.; Glaser, D.; Sonnenfeld, R.; Drake, R.; Hansma, P. K.; Elings, U. *J. Vac. Sci. Technol., A* **1988**, *6*, 283. (d) Schneir, J.; Elings, V.; Hansma, P. K. *J. Electrochem. Soc.*, in press. (e) Schneir, J.; Hansma, P. K.; Elings, V.; Gurley, J.; Wickramasinghe, K.; Sonnenfed, R. *Proc. Soc. Photo-Opt. Instrum. Engl.*, in press.
(7) (a) Liu, H. Y.; Fan, F.-R. F.; Lin, C. W.; Bard, A. J. *J. Am. Chem. Soc.* **1986**, *108*, 3838. (b) Fan, F.-R.; Bard, A. J. *Anal. Chem.* **1988**, *60*, 75.
(8) Itaya, K.; Higaki, K.; Sugawara, S. *Chem. Lett.* **1988**, 421.
(9) Lev, O.; Fan, F.-R. F.; Bard, A. J. *J. Electrochem. Soc.* **1988**, *135*, 783.
(10) Lustenberger, P.; Rorher, H.; Christoph, R.; Siegenthaler, H. *J. Electroanal. Chem.* **1988**, *243*, 225.
(11) Wiechers, J.; Toomey, T.; Kolde, B. M.; Behm, R. J. *J. Electroanal. Chem.*, in press.
(12) (a) Besenhard, J. O.; Fritz, H. P. *Angew. Chem., Int. Ed. Engl.* **1983**, *22*, 950, and references therein. (b) Kinoshita, K. *Carbon: Electrochemical and Physiochemical Properties*; Wiley: New York, 1988.
(13) Besenhard, J. O.; Theodoridon, E.; Mohwald, H.; Nickl, J. J. *Synth. Met.* **1982**, *4*, 211.
(14) (a) Proctor, A.; Sherwood, P. M. A. *Carbon* **1983**, *21*, 53. (b) Takahaqi, T.; Ishitani, A. *Carbon* **1984**, *22*, 43. (c) Kozlowski, C.; Sherwood, P. M. A. *J. Chem. Soc., Faraday Trans. 1* **1985**, *81*, 2745. (d) Kamau, G. N.; Lollis, W. S.; Riesling, J. F. *Anal. Chem.* **1985**, *57*, 545. (e) Poon, M.; McCreary, R. L. *Anal. Chem.* **1986**, *58*, 2754.
(15) Kaiser, W. J.; Jaklevic, R. C. *Rev. Sci. Instrum.* **1988**, *59*, 537.
(16) Drake, B.; Sonnenfeld, R.; Schneir, J.; Hansma, P. K. *Surf. Sci.* **1987**, *181*, 92.
(17) Binnig, G.; Smith, D. P. E. *Rev. Sci. Instrum.* **1986**, *57*, 1688.
(18) Park, S.-L.; Quate, C. F. *Rev. Sci. Instrum.* **1987**, *58*, 2010.
(19) Hansma, P. K.; Tersoff, J. *J. Appl. Phys.* **1987**, *61*, R1.
(20) *Analog Devices 1984 Databook*, Vol. 1, pp 20-77.

0022-3654/88/2092-5563$01.50/0

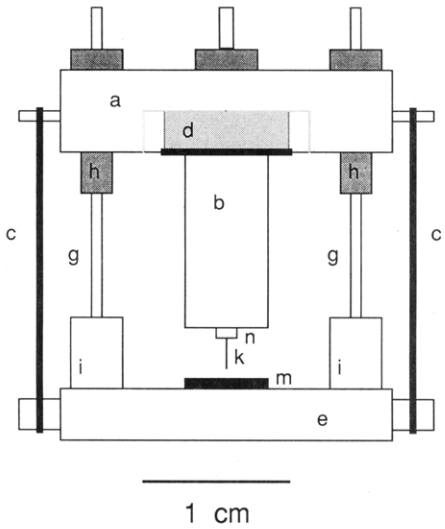

Figure 1. Design of the STM used in this study: (a) steel support plate; (b) piezoceramic tube scanner; (c) Viton O-ring bands; (d) piezo for thermal drift compensation; (e) glass sample plate; (g) 4-80 stainless steel threaded rod; (h) brass holders; (i) glass cups; (k) tip; (m) Kel-F and Teflon sample holders; (n) tip holder. Scale is indicated.

universal programmer. The auxiliary electrode was a 1.5-cm^2 Pt flag. Barrier height measurements were made by modulating the tip–sample distance by 0.5 Å at 15 kHz, locking in on the tunneling current by using a PAR 5206 lock-in amplifier equipped with a Model 5048 Lin/Log Ratiometer and recording $d(\log i)/ds$, where i is the tunneling current and s the tip-to-sample distance. Data acquisition was with an IBM PC-AT computer equipped with a Keithly Series 500 interface. The barrier height, ϕ, was then obtained via the Fowler–Nordheim relationship where $\phi = [(d(\log i)/ds)/1.025]^2$.

The STM tip was made by electrochemically etching a 125-μm Pt–Ir rod to a point and coating with insulating varnish (Epoxylite 6001, Epoxylite Corp., Irvine, CA). This insulation minimizes the faradaic contribution to the tip current and leaves an estimated bare metal area of ca. 10 000 $Å^2$.[21]

Highly oriented pyrolytic graphite was obtained from Dr. Arthur Moore of Union Carbide Corp., Parma, OH. Electrical connection to the sample was made by attaching a copper wire to the material with silver paint and then covering the entire wire and contact with Torr-Seal epoxy cement (Varian, Lexington, MA). The edges of the sample were sealed with silicone rubber adhesive sealant (GC Electronics, Rockford, IL), leaving an exposed sample area of about 0.2 cm^2. H_2SO_4 was reagent grade and aqueous solutions were prepared with Millipore water.

STM images were obtained with the HOPG sample +0.05 V vs AgQRE, with the tip biased −50 mV relative to the virtually grounded HOPG working electrode. Thus, the tip potential was 0.00 V vs AgQRE, which is the double-layer region for Pt. At this potential the faradaic current at the tip was always less than 0.1 nA before electrochemical cycling. Note that appropriate biasing of the substrate and tip is useful in adjusting the tip potential to be in a region where it is stable and where the tip faradaic current is minimized.[22] If the tip potential was left fixed at −50 mV relative to the sample during electrochemical cycling of the sample to +1.8 V vs AgQRE, a large (>100-nA) anodic current at the tip was observed, because, under these conditions, the tip was driven to very positive potentials. This anodic current represents oxidation of water at the exposed Pt with the evolution of oxygen and perhaps a contribution from the oxidation of the carbonaceous protective coating on the tip. Under these conditions the electrochemical cycling removed or altered the coating; after five cycles the background current increased to >2 nA with the tip 0.0 V vs AgQRE. One way to eliminate the electrochemical processes at the tip is to ramp the tip voltage simultaneously with the potential sweep of the sample,[10] thus keeping the tip at 0.0 V vs AgQRE. An alternative method, which we used for these experiments, was to back the tip ca. 25 μm from the surface and disconnect it during electrochemical cycling of the sample, allowing it to equilibrate with the solution potential. With this procedure background currents at the tip never exceeded 1 nA, even after 100 cycles of the HOPG.

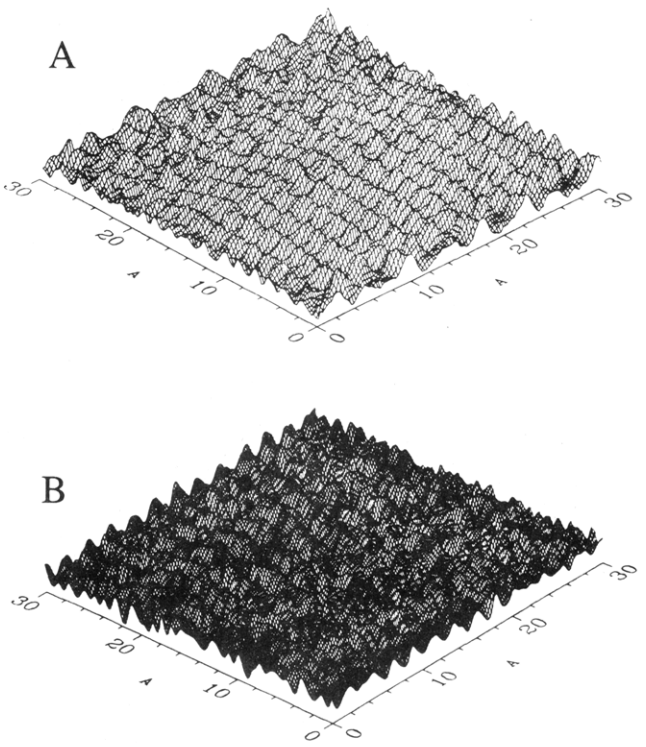

Figure 2. Constant-height STM images of highly oriented pyrolytic graphite in (A) air and (B) 0.1 M H_2SO_4 with the sample held at 0.05 V vs AgQRE. $V_{tip} = -50$ mV, $i_{tunnel} = 5$ nA. Scan speed was 780 Å/s and the corrugation amplitude was 1.2 nA.

Results and Discussion

Constant-height images of the atomic surface structure of graphite in air and in 0.1 M H_2SO_4 at 0.05 V vs AgQRE are shown in Figure 2. In these images the tunneling current was 5 nA (with 0.02-nA background in solution) and the tip bias was −50 mV, yielding a tunneling resistance of 10^7 ohms. While the resolution of the image observed in air is somewhat better than that in solution, our ability to obtain these images does demonstrate that atomic resolution images in solution are achievable with reasonable tunneling resistances and with the sample under potential control. The reduction in image quality in aqueous solution when coated tips are used may be a result of some residual insulation remaining on the tip. Of particular note in the image obtained in air is a disordered region where the lattice appears to go through a kink; as discussed below, these kink sites appear to be important in the way the surface oxidizes during anodization.

A 600- × 600-Å constant-current STM image of the HOPG surface in 0.1 M H_2SO_4 at 0.05 V vs AgQRE is shown in Figure 3A. Consistent with a previous report[14] in a different electrolyte, this surface is atomically flat over large areas. An additional measure of the smoothness and lack of contamination of these surfaces, even in electrolyte solution, is the featureless barrier height $(d(\log i)/ds)$ (Figure 3B) during the scan to record the topographic image. The barrier height to tunneling was 0.9 eV, consistent with that found previously in a vacuum.[23] These images were stable for several hours at 0.05 V vs AgQRE, and atomic resolution could be obtained at any time with the potential held

(21) (a) Gewirth, A. A.; Craston, D. H.; Bard, A. J., to be published. (b) Wightman, R. M. In *Electroanalytical Chemistry*; Bard, A. J., Ed.; Marcel Dekker: New York, 1988; Vol. 15.

(22) Bard, A. J.; Lev, O.; Fan, F.-R. F. Presented at the 194th Meeting of the American Chemical Society, New Orleans, LA, 1987.

(23) Binnig, G.; Rohrer, H. *IBM J. Res. Dev.* **1986**, *30*, 355.

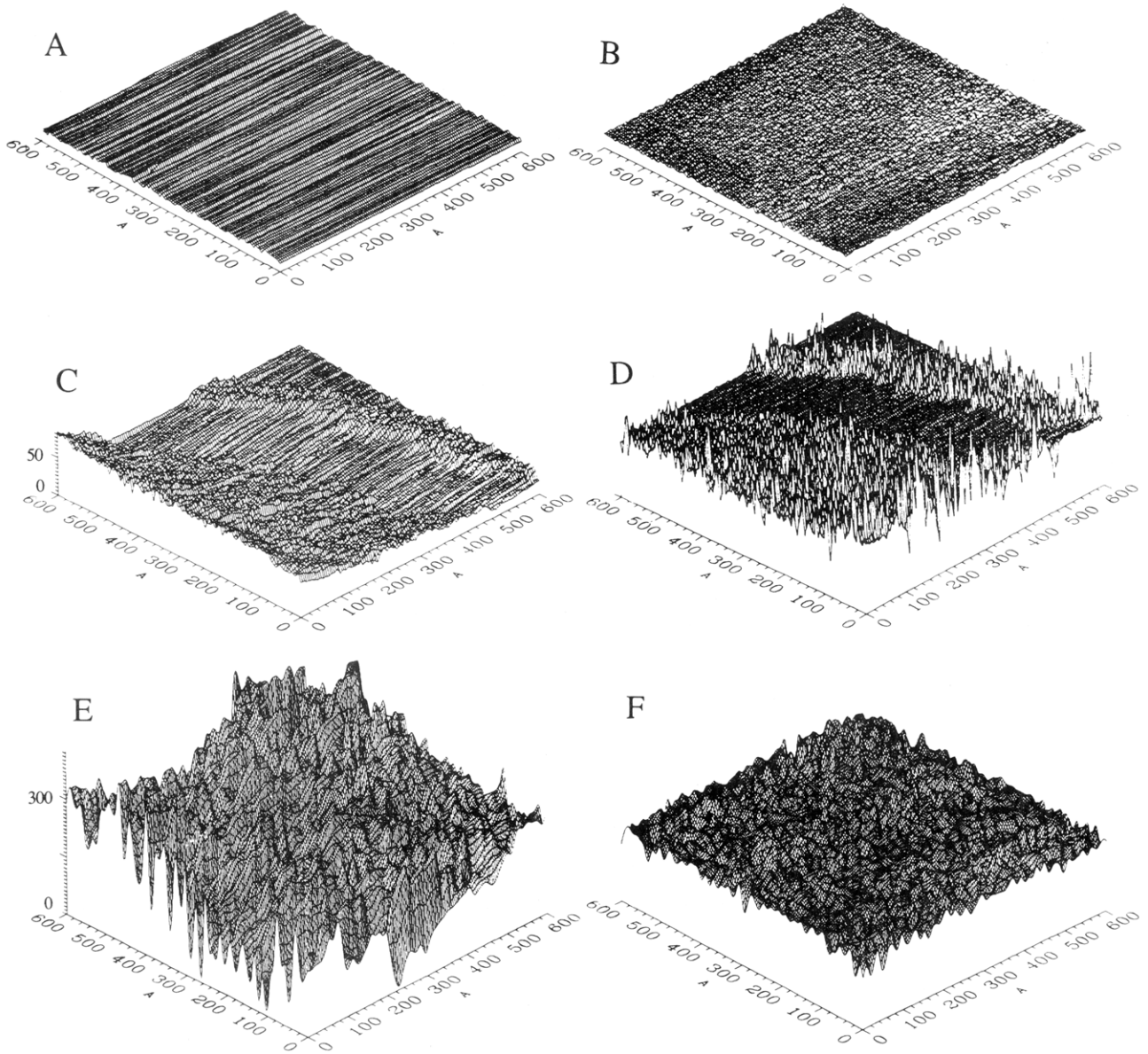

Figure 3. Constant-current STM images (A, C, E) and d(log i)/ds scans of the same areas (B, D, F) of the anodic oxidation of highly oriented pyrolytic graphite in 0.1 M H_2SO_4 at 0.05 V vs AgQRE. V_{tip} = −50 mV, i_{tunnel} = 7 nA. Scan speed was 260 Å/s. (A) HOPG topograph before oxidation and (B) corresponding barrier height measurement (barrier height, 0.9 eV). (C) HOPG topograph after 20 potential cycles and (D) corresponding barrier height. (Barrier height decreases in the upward directions.) (E) HOPG topograph after further oxidation of the surface and (F) corresponding barrier height.

at this value. This implies the HOPG surface is quite inert and does not absorb or intercalate material from the solution at this potential.

Cycling the potential of the HOPG electrode between 0.0 and 1.8 V vs AgQRE at 200 mV/s yielded cyclic voltammograms showing the characteristic oxidation wave at 1.8 V and a slightly diminished reduction peak at 1.5 V. The oxidation wave has been attributed to a combination of graphite oxidation and the intercalation of HSO_4^- into the graphite lattice. The oxidation of graphite is chemically (but not thermodynamically) reversible, and the reduction wave is attributed[24] (a) to reduction of graphitic oxide and (b) to deintercalation of HSO_4^-. In dilute acid solutions, such as that used here, the redox process is less reversible; during the oxidation process the graphite structure is thought to be disturbed, with bonds on the surface broken (possibly due to hydrolysis) and a residual, partially insulating, oxide overlayer, which is stable at 0.05 V vs AgQRE, formed.[25]

After 10 cycles STM images at this potential showed widely scattered irregular protrusions between 20 and 30 Å high and about 100 Å^2 in area growing out of the flat HOPG background. Atomic resolution was still obtainable in the flat areas, indicating that no adsorption or surface modification had taken place there. In contrast, the protruded regions showed greatly diminished barrier heights (less than 0.25 eV) and no resolved atoms. A similar effect was observed by Sonnenfeld and Schardt in their study of Ag deposition on graphite.[4]

After another 10 potential cycles, the islands of surface corrugation grew together anisotropically giving STM topographic images such as that shown in Figure 3C. Flat areas of unoxidized graphite, with barrier heights (Figure 3D) of ca. 0.9 eV, were interleaved with channels of rough, oxidized areas. These channels showed reduced barrier heights consistent with the formation of a more insulating layer (less charge on the surface and more charge tightly held) growing into the bulk. As before, atomic resolution of the characteristic graphite structure is possible in the flat regions, indicating that no overlayer was formed on the smooth graphite.

Finally, another 10 potential sweeps gave rise to very rough topographs, as shown in Figure 3E, which, however, showed

(24) Beck, F.; Krohn, H. *Synth. Met.* **1983**, *7*, 193.
(25) (a) Besenhard, J. O.; Fritz, H. P. *Z. Anorg. Allg. Chem.* **1975**, *416*, 106. (b) Besenhard, J. O.; Wudy, E.; Mohsald, H.; Nickl, J. J.; Bibenacher, W.; Foag, W. *Synth. Met.* **1983**, *7*, 185.

relatively flat, but low, barrier heights as shown in Figure 3F. The surface was now completely oxidized, and the exposed surface, after removal from the solution, appeared covered with a grayish film. This film has previously been associated with surface oxidation.[26]

The STM images presented above suggest that the formation of a graphitic oxide overlay occurs according to a nucleation and growth mechanism. The irreversible breaking of C–C bonds and the formation of graphitic oxide overlayer in the dilute acid environment studied here probably occur initially at step and defect sites (such as seen in Figure 2A) on the otherwise flat HOPG surface. The oxidation proceeds most rapidly along step and ridge sites and at a somewhat slower rate into the basal plane. The basal plane is unaffected by the cycling until the oxide grows in from initial defect sites. The oxide overlayer formed through this anodic procedure exhibits a barrier height that is substantially lower than that found for the bare HOPG surface, which is consistent with its more insulating nature. This overlayer is also amorphous and loses the layer structure present in unoxidized HOPG.

This study illustrates the utility of the STM for following in situ progress of electrochemical reactions. We have demonstrated that atomic resolution is obtainable under potential control. Simultaneous barrier height measurements have proven useful in following the appearance of an overlayer structure and should, in general, have utility in following the progress of electrochemical reactions on electrode surfaces. With slightly improved resolution, images of atoms on metal surfaces[27] might be possible, enabling study of a wide variety of electrochemical processes with the STM.

Acknowledgment. Support of this research by the Texas Advanced Technology Research Program is gratefully acknowledged. We thank Derek H. Craston, Fu-Ren F. Fan, and Larry J. Kepley for helpful discussions and Arthur W. Moore for providing HOPG.

(26) Kepley, L. J.; Bard, A. J. *Anal. Chem.* **1988**, *60*, 1459.

(27) Hallmark, U. M.; Chang, S.; Rabolt, J. F.; Sualen, J. D.; Wilson, R. J. *Phys. Rev. Lett.* **1987**, *59*, 2879.

Electrogenerated Chemiluminescent Emission from an Organized (L–B) Monolayer of a $Ru(bpy)_3^{2+}$-Based Surfactant on Semiconductor and Metal Electrodes

Xun Zhang and Allen J. Bard*

Department of Chemistry, The University of Texas, Austin, Texas 78712 *(Received: May 31, 1988)*

Electrogenerated chemiluminescence (ECL) from an organized monomolecular layer of a surfactant derivative of $Ru(bpy)_3^{2+}$ consisting of a single stearamidomethylene chain linked to one bipyridine unit at the 4-position and abbreviated $Ru(bpy)_2(bpy\text{-}C_{19})^{2+}$ has been observed at the surfaces of In-doped tin oxide, Pt, and Au electrodes. The surfactant monolayer was coated on the substrate electrodes by the Langmuir–Blodgett method. ECL was generated in an electrochemical cell containing an aqueous oxalate solution by applying a positive potential to the electrode modified by the monolayer of $Ru(bpy)_2(bpy\text{-}C_{19})^{2+}$. The ECL of the emitter monolayer deposited on an In-doped SnO_2 electrode was quite intense with an emission maximum at ca. 680 nm. The ECL of the monolayer deposited on Pt and Au electrodes was generally 10^2–10^3 times weaker than that on SnO_2, but still easily detectable.

We report here the first observation of the electrogenerated chemiluminescence (ECL)[1] from a monomolecular layer of emitter molecules confined to the surface of a solid electrode. The emitter employed was a surfactant derivative of tris(bipyridine)ruthenium complex, which was deposited on smooth metal or semiconductor electrodes as an organized assembly by the Langmuir–Blodgett (L–B) method

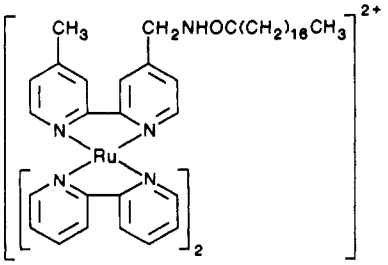

$Ru(bpy)_2(bpy\text{-}C_{19})^{2+}$ (I)

The observed luminescent emission was generated from the coated electrodes placed in aqueous oxalate solutions and biased to positive potentials. ECL has been generated in a variety of electrochemical systems, including polymer films on electrode surfaces.[2] The ECL of the $Ru(bpy)_3^{2+}/C_2O_4^{2-}$ in aqueous media arises from the oxidation of $Ru(bpy)_3^{2+}$ at an electrode in the presence of oxalate by the following proposed reaction sequence:[3]

$$Ru(bpy)_3^{2+} \rightarrow Ru(bpy)_3^{3+} + e \quad (1)$$

$$Ru(bpy)_3^{3+} + C_2O_4^{2-} \rightarrow Ru(bpy)_3^{2+} + C_2O_4^{-} \quad (2)$$

$$C_2O_4^{-} \rightarrow CO_2 + CO_2^{-} \quad (3)$$

$$Ru(bpy)_3^{2+} + CO_2^{-} \rightarrow Ru(bpy)_3^{+} + CO_2 \quad (4)$$

$$Ru(bpy)_3^{3+} + Ru(bpy)_3^{+} \rightarrow Ru(bpy)_3^{2+*} + Ru(bpy)_3^{2+} \quad (5)$$

$$Ru(bpy)_3^{3+} + CO_2^{-} \rightarrow Ru(bpy)_3^{2+*} + CO_2 \quad (6)$$

This ECL system was found useful in the determinations of both $Ru(bpy)_3^{2+}$ and oxalate at low concentration levels.[4]

There have also been studies of the synthesis of surfactant derivatives of $Ru(bpy)_3^{2+}$ and their photochemical properties in solution and as organized monolayer assemblies.[5,6] The reported luminescent emission of such surfactant monolayers, however,

* Author to whom correspondence should be addressed.

(1) See, for example: (a) Bard, A. J.; Faulkner, L. R. In *Electroanalytical Chemistry*; Bard, A. J., Ed.; Dekker: New York, 1977, Vol. 10, and references therein. (b) Faulkner, L. R. In *MTP International Review of Science: Physical Chemistry Series Two*; Herschbach, D. R., Ed.; Butterworths: London, 1976, Vol. 9, p 213, and references therein. (c) Bard, A. J.; Faulkner, L. R. *Electrochemical Methods*; Wiley: New York, 1980; pp 621–629.

(2) Rubinstein, I.; Bard, A. J. *J. Am. Chem. Soc.* (a) **1980**, *102*, 6641; (b) **1981**, *103*, 5007.

(3) (a) Chang, M.; Saji, T.; Bard, A. J. *J. Am. Chem. Soc.* **1977**, *99*, 5399. (b) Rubinstein, I.; Bard, A. J. *Ibid* **1981**, *103*, 512.

(4) (a) Ege, D.; Becker, W. G.; Bard, A. J. *Anal. Chem.* **1984**, *56*, 2413. (b) Rubinstein, I.; Martin, C. R.; Bard, A. J. *Ibid.* **1983**, *54*, 1580.

(5) Sprintschnik, G.; Sprintschnik, H. W.; Kirsch, P. P.; Whitten, D. G. *J. Am. Chem. Soc.* (a) **1976**, *98*, 2337; (b) **1977**, *99*, 4947.

(6) Kalyanasundaram, K. *Coord. Chem. Rev.* **1982**, *46*; 218–224 and references therein (ref 257–265).

0022-3654/88/2092-5566$01.50/0